Vibration Mode Identification and Coupling Assessment with the Mindlin Plate Equations and Measurements in a Quartz Crystal Plate

Qiaoqiao Pan[1], Ji Wang[2], Shih-Yung Pao[1], Min-Chiang Chao [1], Julian Shen[1]
[1] TXC (Ningbo) Corporation, Beilun District, Ningbo, Zhejiang 315800, CHINA
[2] Piezoelectric Device Lab, School of Mech Eng & Mechanics, Ningbo University, Ningbo, Zhejiang 315211, CHINA
E-mail: wangji@nbu.edu.cn, chaomk@txc.com.tw

***Abstract*—In the design of quartz crystal resonators, it is always required to have complete information about vibration couplings in the vicinity of thickness-shear mode for the suppression of spurious modes which always cause performance degradation as one of the most serious challenges in product development. The couplings of vibration modes are caused by the finite size of plates and material constants, while the effect is shown as occurrences of vibration near the primary resonance of thickness-shear vibration. The analysis of high frequency vibrations of quartz crystal plates has been done with the Mindlin plate theory with accurate solutions of the frequency and mode shapes for the identification of couplings of modes in relatively complicated frequency spectra. We have been using with the first-order Mindlin plate equations based on straight-crested wave assumptions for the frequency and mode shape solutions in both plane directions. We found the majority of spurious modes in the neighborhood of thickness-shear mode have been identified, then we can predict their movements with variations of plate and electrodes configurations and temperature changes. By measuring strong couplings of vibration modes in the vicinity of thickness-shear frequency of a crystal plate, we can obtain complete frequency spectra within the given band. Our calculations from a finite set of vibrations modes from truncated Mindlin plate equations are demonstrating the effectiveness in the analysis because the major couplings have been predicted in good agreement with measurements. It offers a promising approach for the improvement of current design procedure based on empirical knowledge.**

Keywords: Mindlin, plate, crystal, vibration, resonator

I. INTRODUCTION

Today, AT-cut quartz resonator suppliers usually receive very strict performance specifications from their customers. These specifications require suppliers to provide resonators which can keep good impedance and frequency characteristics in a very long temperature span. At the same time, the resonator's miniaturization also increases the difficulty of manufacturing. Therefore, designers turn to plate theory to direct their design and analysis process with the objective of reducing their experimental time and cost.

There is quite a long history in plate theory. Mindlin did a series of work in crystal plate vibration as the foundation of AT-cut quartz resonator analysis [1-3]. Lee et al constructed an FEA program based on Mindlin's 2D theory to analyze pure mechanical crystal plate vibration without piezoelectric effects [4]. Yong and Wang extended the work and offered some details like frequency-temperature characteristics and quality factor [5-6]. Today, many commercial FEA software could also simulate quartz plate vibrations. Undoubtedly FEM is a powerful tool, however, it often comes out much more modes than we expected to see. It is time consuming to separate modes from each other and figure out the important modes we need to pay attention to in the resonator design process.

In this paper, we still choose to follow Mindlin 2D plate theory to calculate frequencies and mode shapes in both plate directions. Then by following Koga and Fukuyo [7], we measured the frequency of AT-cut quartz crystal plates of different lengths. Next, the calculated frequency spectrum is compared with measured spectrum, and their differences and similarities are observed. This work can help to increase the accuracy of plate theory. It also could be used for the verification of FEM results and provide meaningful information that which mode is worth paying attention to. We hope current efforts in cross checking of measurements and analytical predictions will improve the design process with more emphasis on computer-based modeling.

II. THE FIRST-ORDER MINDLIN PLATE EQUATIONS

Consider an AT-cut rectangular plate of thickness *2b*, length *2a* and width *2c*, as shown in Fig. 1. The axis x_1 coincides with diagonal axis of the quartz crystal and x_3 makes an angle of 35°15' with the trigonal axis. Following Ref. [3], we use the first-order Mindlin plate theory to calculate the mode shapes and frequencies of a plate. The equations of motion are:

$$T_{1,1}^{(0)} + T_{5,3}^{(0)} = 2b\rho\ddot{u}_1^{(0)},$$

$$T_{6,1}^{(0)} + T_{4,3}^{(0)} = 2b\rho\ddot{u}_2^{(0)},$$

$$T_{5,1}^{(0)} + T_{3,3}^{(0)} = 2b\rho\ddot{u}_3^{(0)};$$

Preprint for 2012 IEEE International Ultrasonics Symposium,
October 7~10, 2012, Dresden, Germany

$$T_{1,1}^{(1)} + T_{5,3}^{(1)} - T_6^{(0)} = \frac{2b^3}{3}\rho\ddot{u}_1^{(1)},$$
$$T_{5,1}^{(1)} + T_{3,3}^{(1)} - T_4^{(0)} = \frac{2b^3}{3}\rho\ddot{u}_3^{(1)}. \quad (1)$$

The stress-displacement relations are:

$$T_1^{(0)} = 2b\left[\bar{c}_{11}u_{1,1}^{(0)} + \bar{c}_{13}u_{3,3}^{(0)} + \kappa_4\bar{c}_{14}(u_{2,3}^{(0)} + u_3^{(1)})\right],$$
$$T_3^{(0)} = 2b\left[\bar{c}_{31}u_{1,1}^{(0)} + \bar{c}_{33}u_{3,3}^{(0)} + \kappa_4\bar{c}_{34}(u_{2,3}^{(0)} + u_3^{(1)})\right],$$
$$T_4^{(0)} = 2\kappa_4 b\left[\bar{c}_{41}u_{1,1}^{(0)} + \bar{c}_{43}u_{3,3}^{(0)} + \kappa_4\bar{c}_{44}(u_{2,3}^{(0)} + u_3^{(1)})\right],$$
$$T_5^{(0)} = 2b\left[c_{55}(u_{1,3}^{(0)} + u_{3,1}^{(0)}) + \kappa_6 c_{56}(u_{2,1}^{(0)} + u_1^{(1)})\right],$$
$$T_6^{(0)} = 2\kappa_6 b\left[c_{65}(u_{1,3}^{(0)} + u_{3,1}^{(0)}) + \kappa_6 c_{66}(u_{2,1}^{(0)} + u_1^{(1)})\right];$$

$$T_1^{(1)} = \frac{2b^3}{3}(\tilde{c}_{11}u_{1,1}^{(1)} + \tilde{c}_{13}u_{3,3}^{(1)}),$$
$$T_3^{(1)} = \frac{2b^3}{3}(\tilde{c}_{31}u_{1,1}^{(1)} + \tilde{c}_{32}u_{3,3}^{(1)}),$$
$$T_5^{(1)} = \frac{2b^3}{3}\hat{c}_{55}(u_{1,3}^{(1)} + u_{3,1}^{(1)}); \quad (2)$$

and

$$\kappa_4^2 = \kappa_6^2 = \frac{\pi^2}{12},$$
$$\bar{c}_{ij} = c_{ij} - \frac{c_{i2}c_{2j}}{c_{22}}, i, j = 1,3,4;$$
$$\tilde{c}_{ij} = c_{ij} - \frac{c_{i4}c_{4j}}{c_{44}}, i, j = 1,2,3; \quad (3)$$
$$\hat{c}_{ij} = c_{ij} - \frac{c_{i6}c_{6j}}{c_{66}}, i, j = 5.$$

Then, the boundary conditions for free edges of plate are:

$$T_1^{(0)} = T_5^{(0)} = T_6^{(0)} = T_1^{(1)} = T_5^{(1)} \text{ on } x_1 = \pm a,$$
$$T_3^{(0)} = T_5^{(0)} = T_4^{(0)} = T_4^{(1)} = T_5^{(1)} \text{ on } x_3 = \pm c. \quad (4)$$

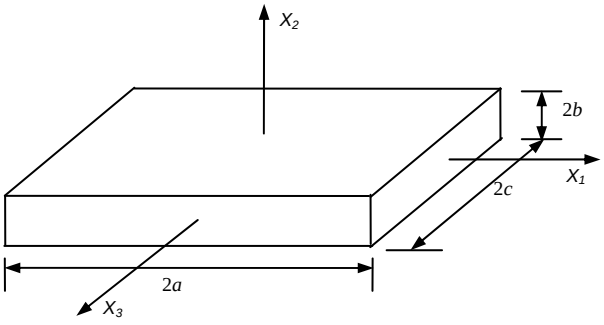

Fig. 1. A rectangular crystal plate with coordinates.

III. The Fundamental Solutions

By substituting (2) into (1), the equations of motion in displacements become:

$$\begin{aligned}
&\bar{c}_{11}u_{1,11}^{(0)} + \bar{c}_{13}u_{3,13}^{(0)} + \kappa_4\bar{c}_{14}(u_{2,13}^{(0)} + u_{3,1}^{(1)}) + \\
&c_{55}(u_{3,13}^{(0)} + u_{1,33}^{(0)}) + \kappa_6 c_{56}(u_{2,13}^{(0)} + u_{1,3}^{(1)}) = \rho\ddot{u}_1^{(0)}, \\
&\kappa_4\bar{c}_{14}u_{1,13}^{(0)} + \kappa_4\bar{c}_{34}u_{3,33}^{(0)} + \kappa_4^2\bar{c}_{44}(u_{2,33}^{(0)} + u_{3,3}^{(1)}) + \\
&\kappa_6 c_{56}(u_{3,11}^{(0)} + u_{1,13}^{(0)}) + \kappa_6^2 c_{66}(u_{2,11}^{(0)} + u_{1,1}^{(1)}) = \rho\ddot{u}_2^{(0)}, \\
&\bar{c}_{13}\bar{u}_{1,13}^{(0)} + \bar{c}_{33}u_{3,33}^{(0)} + \kappa_4\bar{c}_{34}(u_{2,33}^{(0)} + u_{3,3}^{(1)}) + \\
&c_{55}(u_{3,11}^{(0)} + u_{1,13}^{(0)}) + \kappa_6 c_{56}(u_{2,11}^{(0)} + u_{1,1}^{(1)}) = \rho\ddot{u}_3^{(0)}; \\
&\tilde{c}_{11}u_{1,11}^{(1)} + \tilde{c}_{12}u_{3,13}^{(1)} + \hat{c}_{55}(u_{3,13}^{(1)} + u_{1,33}^{(1)}) - \\
&3b^{-2}[\kappa_6 c_{56}(u_{1,3}^{(0)} + u_{3,1}^{(0)}) + k_6^2 c_{66}(u_{2,1}^{(0)} + u_1^{(1)})] = \rho\ddot{u}_1^{(1)}; \\
&\hat{c}_{55}(u_{1,31}^{(1)} + u_{3,11}^{(1)}) + \tilde{c}_{31}u_{1,13}^{(1)} + \tilde{c}_{32}u_{3,33}^{(1)} - \\
&3b^{-2}[\kappa_4\bar{c}_{14}u_{1,1}^{(0)} + \kappa_4\bar{c}_{34}u_{3,3}^{(0)} + \kappa_4^2\bar{c}_{44}(u_{2,3}^{(0)} + u_3^{(1)})] = \rho\ddot{u}_3^{(1)}.
\end{aligned} \quad (5)$$

Therefore, the fundamental solutions of (5) can be:

$$\begin{aligned}
u_1^{(0)} &= P_1\cos(\xi x_1 + r\pi/2)\sin(\zeta x_3 + s\pi/2)e^{i\omega t}, \\
u_2^{(0)} &= P_2\sin(\xi x_1 + r\pi/2)\cos(\zeta x_3 + s\pi/2)e^{i\omega t}, \\
u_3^{(0)} &= P_3\sin(\xi x_1 + r\pi/2)\cos(\zeta x_3 + s\pi/2)e^{i\omega t}, \\
u_1^{(1)} &= P_4\cos(\xi x_1 + r\pi/2)\cos(\zeta x_3 + s\pi/2)e^{i\omega t}, \\
u_3^{(1)} &= P_5\sin(\xi x_1 + r\pi/2)\sin(\zeta x_3 + s\pi/2)e^{i\omega t},
\end{aligned} \quad (6)$$

where r = 0 or 1 and s = 0 or 1. However if we use the (6) to describe mode's displacement to satisfy boundary conditions, simple closed solutions may not be found. Mindlin and Gazis[3] provided their method to simplify solutions.

IV. Solutions A and B

In order to find simple closed solutions to satisfy boundary condition (7) or (8), we simplify (6) to get approximate results.

For solution A, displacements $u_1^{(0)}$, $u_2^{(0)}$ and $u_1^{(1)}$ have been taken into account for face-shear, flexure, and thickness-shear modes. Therefore (6) may be written as:

$$\begin{aligned}
u_2^{(0)} &= A_1\sin\xi x_1 e^{i\omega t}, \\
u_1^{(1)} &= \frac{A_2}{b}\cos\xi x_1 e^{i\omega t}, \\
u_3^{(0)} &= A_3\sin\xi x_1 e^{i\omega t}, \\
u_1^{(0)} &= u_3^{(1)} = 0.
\end{aligned} \quad (7)$$

where $A_i (i = 1,2,3); \xi, \omega$ and t are vibration amplitudes, wavenumber, frequency, and time, respectively. And the boundary conditions (7) become:

$$T_5^{(0)} = T_6^{(0)} = T_1^{(1)} = 0, \text{on } x_1 = \pm a. \quad (8)$$

Because only the displacement change in x_1 axis has been considered, the item 2 of (4) has been ignored.

With displacement (7), displacement equations of motion (5) and boundary condition (8), we can calculate mode shapes and frequency spectra of these three modes.

For solution B, taking displacements $u_1^{(0)}$ and $u_1^{(1)}$ into account for face-shear and thickness-shear vibrations, (6) can be written as:

$$u_1^{(0)} = B_1 \sin \zeta x_3 e^{i\omega t},$$
$$u_1^{(1)} = \frac{B_2}{b} \cos \zeta x_3 e^{i\omega t}, \tag{9}$$
$$u_2^{(0)} = u_3^{(0)} = u_3^{(1)} = 0.$$

For solution A, boundary conditions become:

$$T_5^{(0)} = T_5^{(1)} = 0, \text{ on } x_3 = \pm c. \tag{10}$$

Using displacements in (9), displacement equations of motion (5) and boundary condition (10), we can also calculate mode shapes and frequency spectra of those two modes.

V. Results from Measurements

Nowadays, size of quartz resonators may be only several percents of old resonators which were produced in Mindlin and Koga's age. In this paper we choose rectangular AT-cut quartz plates whose dimensions are about 2.0*1.3mm, which is quite smaller than Koga and Fukuyo's experiment [7]. And, this size is a typical dimension of quartz plates manufactured in these days. The frequency of sample resonators' thickness-shear mode is centered at 41.280MHz. For the measurement, we use a network analyzer to measure the impedance of samples in different frequency spans. Every peak of impedance curves has been recorded and drawn on the frequency spectra as shows in Fig. 2.

In Fig. 2, it can be found that face-shear mode of x_3 matches quite well with calculated results and flexural mode also can be found matches well at the division of each flexural overtone and trend of frequency change along x_1 axis. That means even the sizes of quartz crystal plates are much smaller than those in Mindlin's age, the calculation method can still predict the frequencies of strong spurious modes accurately, and can be used in product design process. However it is also obvious that there is a distance between calculation and measurement results. This is a serious problem which should be solved before applying the analytical method to practical design process.

Moreover, there is a group of frequencies obtained by measurement between two overtones of flexure, whether it belongs to face-shear of x_1 or another kind of modes needs to be identified further.

The mode shapes are also calculated as shown in Figs. 3-5. It can be used to distinguish which kind of modes these frequencies belong to.

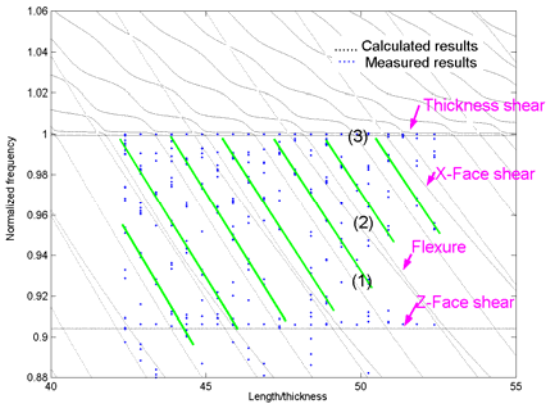

Fig. 2. Calculated and measured resonant frequency spectra

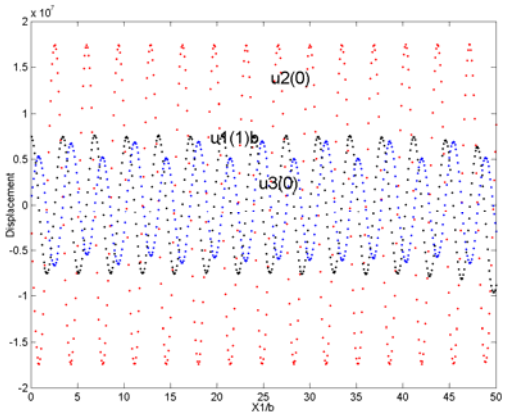

Fig. 3. Calculated displacements of $u_2^{(0)}, u_3^{(0)}$ and $u_1^{(1)}$ in x_1 direction at the frequency of Point 1 in Fig. 2.

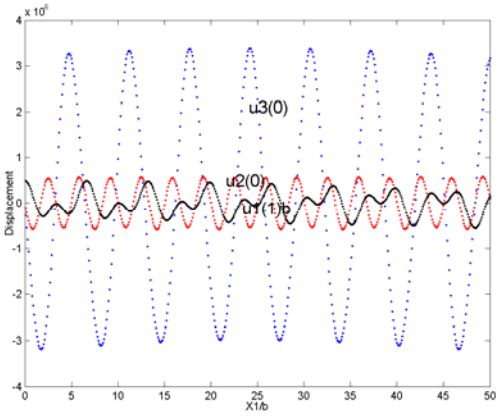

Fig. 4. Calculated displacements of $u_2^{(0)}, u_3^{(0)}$ and $u_1^{(1)}$ in x_1 direction at the frequency of Point 2 in Fig. 2.

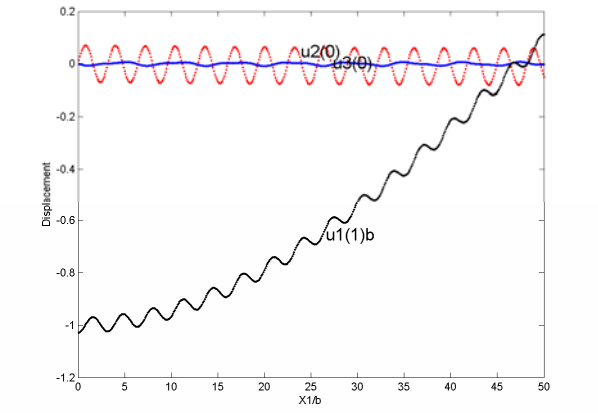

Fig. 5. Calculated displacements of $u_2^{(0)}, u_3^{(0)}$ and $u_1^{(1)}$ in x_1 direction to the frequency of Point 3 in Fig. 2.

VI. Conclusions

With the first-order Mindlin plate theory, the frequency spectrum and mode shapes of strong resonances have been calculated. And we also get an actual frequency spectrum by measuring the quartz plate samples' impedance through frequency sweeping. Comparison of the measured and calculated spectra we found face-shear mode of x_3 matches quite well with calculated results and flexure mode also can be found matches well at the division of each flexure overtone. But there are still some problems which should be solved before applying to practical design process. First one is the distance between calculation and measurement. Second one is that there is a group of frequencies between two overtones of flexure mode in measurement data, and whether it belongs to face-shear of x_1 or another kind of modes needs to be investigated. Finally, the Mindlin plate theory offers a promising approach for the improvement of current design procedure.

Acknowledgments

This project is carried out as an industrial collaboration supported by a grant from TXC (Ningbo) Corporation.

References

[1] R.D. Mindlin, "High frequency vibrations of plated, crystal plates," *Progress* in *Applied Mechanics*, The Prager Anniversary Volume, Macmillan, New York, pp. 73–84, 1963.

[2] R.D. Mindlin and W.J. Spencer, "Anharmonic, thickness-twist overtones of thickness-shear and flexural vibration of rectangular, AT-cut quartz plates," *The Journal of the Acoustical Society of America*, vol. 42, no. 6, pp 1268-1277, 1967.

[3] R.D. Mindlin and D. C. Gazis, "Strong resonances of rectangular AT-cut quartz plates," *Proceedings of the fourth U.S. National congress of Applied Mechanics*, pp 305-310, 1962.

[4] P.C.Y. Lee, C. Zee, and C.A. Brebbia, "Thickness-shear, thickness-twist, and flexural vibration of rectangular AT-cut quartz plates with patch electrodes," in *Proc. of Freq. Control Symp.*, pp 108-119, 1978.

[5] J. Wang, Y.K. Yong, and T. Imai, "High order plate theorey based finite element analysis of the frequency-temperature relations of quartz crystal resonators," in *Proc. of Freq. Control Symp.*, pp 956-963, 1998.

[6] Y.K. Yong, W. Wei, M. Tanaka, and T. Imai, "Three dimensional finite elements and their relationships to Mindlin's higher order plate theory in quartz crystal plate," in *Proc. of Freq. Control Symp.*, pp 791-794, 2001.

[7] I. Koga and H. Fukuyo, "Vibration of thin piezolelctric quartz plate (especially on R1-cut (AT-cut) rectangular plate)," *J. Inst. Elec. Comm. Engrs. of Janpan*, vol. 36, no. 59, 1953. (*In Japanese*)

[8] R.D. Mindlin, "High frequency vibration of piezoelectric crystal plates," *Int. J. Solids Structures*, vol. 8, pp 895-906, 1972.

[9] J. Wang and W. Zhao, "The Determination of the Optimal Length of Crystal Blanks in Quartz Crystal Resonators," *IEEE Tran. on UFFC*, vol. 52, no. 11, pp 2023-2030, 2005.